Dalton Transactions

Cite this: *Dalton Trans.*, 2011, **40**, 10927

www.rsc.org/dalton

PAPER

Thiolato gold(I) complexes containing water-soluble phosphane ligands: a characterization of their chemical and biological properties†

Elena Vergara,[a] Elena Cerrada,[a] Catherine Clavel,[b] Angela Casini*[b] and Mariano Laguna*[a]

Received 12th May 2011, Accepted 8th August 2011
DOI: 10.1039/c1dt10892a

A series of thiolate gold(I) derivatives bearing water soluble phosphanes – namely sodium triphenylphosphane monosulfonate (TPPMS), sodium triphenylphosphane trisulfonate (TPPTS), 1,3,5-triaza-7-phosphaadamantane (PTA) and 3,7-diacetyl-1,3,7-triaza-5-phosphabicyclo[3.3.1]nonane (DAPTA) – is reported and the compounds studied for their luminescence properties in the solid state. Two of these derivatives, [Au(SMe$_2$pyrim)(PTA)] and [Au(SBenzoxazole)(DAPTA)], are also structurally characterized by X-ray diffraction analysis. Strong antiproliferative effects are observed for most of the compounds in the human ovarian carcinoma cell lines (A2780/S) and its cisplatin-resistant variant (A2780/R), which depend on both the type of thiolate and phosphane ligands. ICP-MS studies were also performed to evaluate the influence of the gold uptake on the cytotoxic potency of the compounds.

Introduction

The use of gold complexes in medicine has been essentially centred in the treatment of rheumatoid arthritis.[1,2] However, during the last few decades many gold derivatives have been investigated for their potential use as anticancer agents,[1,3–7] mainly due to the favourable properties of the gold centre and peculiar reactivity with biomolecules with respect to classical Pt(II) anticancer drugs known to possess DNA alkylating properties.[8]

Investigations on the cytotoxicity scores of gold(I) complexes have been focused mainly on auranofin (1-thio-β-D-glucopyranose-2,3,4,6-tetraacetato-S)(triethylphosphine) gold(I)) and its analogues, which present linear gold phosphane thiolate structures.[7] However, a variety of gold(III) derivatives have also been tested as potential antitumor agents, including organogold derivatives, complexes with polydentate ligands, gold porphyrins, gold dithiocarbamates and dinuclear μ-oxo derivatives.[9–13] The mechanisms of action of anticancer gold(I) and gold(III) complexes appear in general to be DNA independent and essentially cisplatin-unrelated.[14] For example, it has been recognised that mitochondria might be critical intracellular target involved in the antitumor activity of the drugs.[15–17] Moreover, several proteins playing relevant functional roles in cells were proposed to represent effective targets for cytotoxic gold compounds, such as thioredoxin reductase, cathepsins, protein tyrosine phosphatase, proteasome, and iodothyronine deiodinase.[12,16–21] Recently, some of us reported on the inhibition of the zinc finger protein poly(ADP-ribose) polymerase (PARP-1) by gold complexes.[22] Interestingly, a recent proteomic study by Messori *et al.* allowed the identification of about 15 proteins showing significant changes in their respective expression rates.[23]

Within this frame, we have described thiolate gold(I) derivatives with the water soluble phosphanes PTA (1,3,5-triaza-7-phosphaadamantane) and DAPTA (3,7-diacetyl-1,3,7-triaza-5-phosphabicyclo[3.3.1]nonane), which display potent cytotoxicity for ovarian, colon, renal and melanoma cancer cell lines in comparison to cisplatin.[24,25] In addition, some of these compounds were screened for their inhibition of mammalian thioredoxin reductases (TrxRs), crucial seleno-enzymes involved in the intracellular redox balance.[12] The results obtained showed that the gold(I)–phosphane complexes efficiently inhibit cytosolic and mitochondrial TrxRs, similarly to auranofin and related compounds.[25] Remarkably, an excellent correlation between cytotoxic properties and TrxR inhibition was outlined.

With the aim of developing new water soluble cytotoxic gold(I) derivatives with anticancer properties, we describe here the synthesis of a series of thiolate gold(I) phosphane complexes bearing sodium triphenylphosphane monosulfonate (TPPMS) and sodium triphenylphosphane trisulfonate (TPPTS) ligands, respectively (Scheme 1). Moreover, some previously reported thiolate gold(I) complexes with PTA and DAPTA ligands,[26] herein further characterized *via* X-ray diffraction analysis, were also studied for their luminescent properties in the solid state. We also include here the preparation of the water soluble gold(I) derivatives of auranofin bearing 1-thio-β-D-glucose tetraacetate and with the PTA and DAPTA ligands replacing the triarylphosphane PEt$_3$.

[a]*Departamento de Química Inorgánica, Instituto de Síntesis Química y Catálisis Homogénea (ISQCH)-C.S.I.C, Universidad de Zaragoza, 50009, Zaragoza, (Spain). E-mail: mlaguna@unizar.es*
[b]*Institut des Sciences et Ingénierie Chimiques, Ecole Polytechnique Fedérale de Lausanne (EPFL), 1015, Lausanne, (Switzerland). E-mail: angela.casini@epfl.ch*

† CCDC reference numbers 790251 and 790252. For crystallographic data in CIF or other electronic format see DOI: 10.1039/c1dt10892a

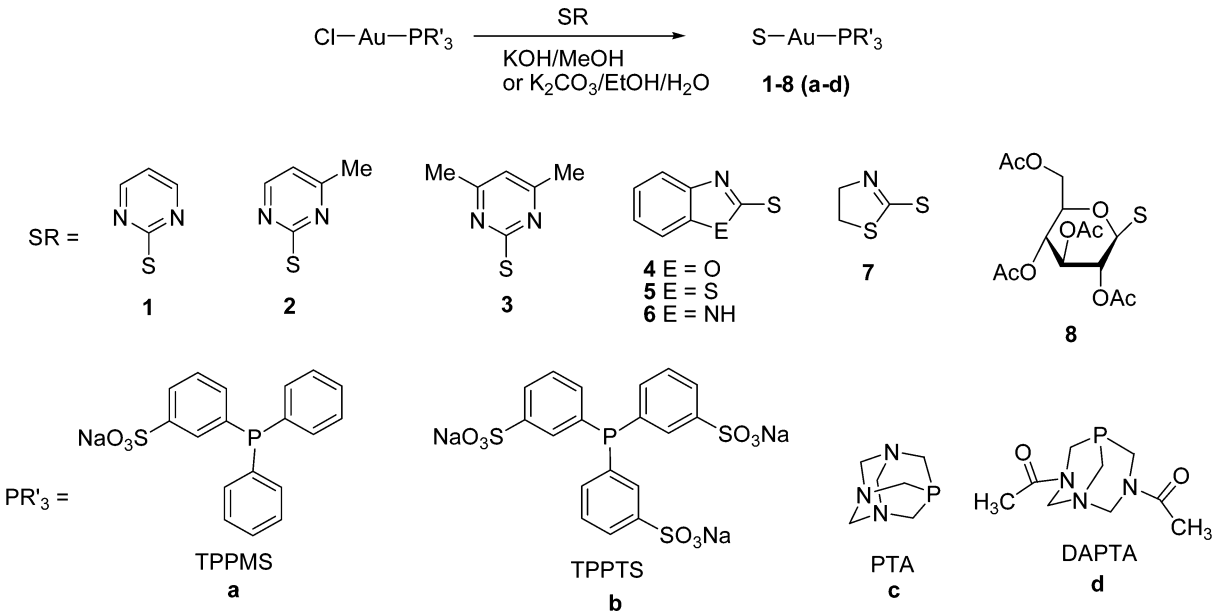

Scheme 1 Preparation of thiolate–gold(I) compounds.

All the compounds have been tested for their antiproliferative activities against human ovarian carcinoma cell lines, and additional cell uptake studies have been conducted in representative cases by inductively coupled plasma mass spectrometry (ICP-MS) to further investigate the differences observed in the cytotoxic properties.

Results and discussion

The synthesis of thiolate gold(I) derivatives **1–8(a–d)** with water soluble phosphanes can be afforded by the addition of the corresponding chloro gold(I) phosphane complex to a solution of the thiol in the presence of a base, as depicted in Scheme 1.

The thiolate gold(I) complexes with sodium triphenylphosphane monosulfonate (TPPMS, **1–7(a)**) and trisulfonate (TPPTS, **1–6(b)**) are isolated as pale yellow solids in good yields. All of them show singlet resonances at about 37 ppm in their $^{31}P\{^{1}H\}$ NMR spectra, displaced to a lower field compared with those of the free phosphanes which appear at *ca.* –6 ppm in both cases. The ^{1}H NMR spectra display, apart from the absence of the S–*H* signal, the characteristic phenyl signals of the phosphane and those due to the thiolate, the latter being high field displaced in the case of the TPPTS derivatives compared with those found in the TPPMS complexes.

Interestingly, in recent years, several examples of carbohydrate compounds have been developed for diverse medicinal applications, ranging from compounds with antibiotic, antiviral, or fungicidal activity and anticancer compounds.[27] Within this frame, we have prepared two thioglucosetetraacetate Au(I) complexes, namely **8c** and **8d**, with PTA and DAPTA ligands, respectively. In fact, it has been shown that 1-thio-β-D-glucose 2,3,4,6-tetraacetate is acting as a true substrate for the glucose active-transport system, and can be used to increase the uptake of metal compounds.[28]

In general, the preparation and characterization of the thiolate derivatives with PTA and DAPTA groups reported herein was previously described by some of us,[24,26] except that in the case of the thioglucosetetraacetate thiolates (see Experimental).

All the described gold compounds are highly water soluble with values ranging from 90 to 480 g L^{-1}. In the case of the TPPMS derivatives, the solubilities are higher than that of the chloro–gold precursors;[29–32] conversely, lower values are found for the TPPTS compounds compared with the starting material.

The crystalline structure of complex [Au(SMe$_2$pyrim)(PTA)] (**3c**) was determined by X-ray diffraction (Fig. 1), and found to

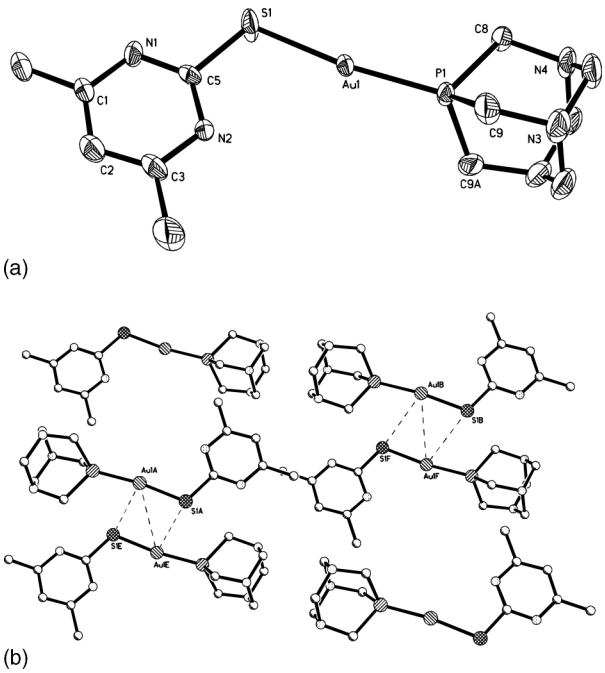

Fig. 1 (a) Molecular structure of [Au(SMe$_2$pyrim)(PTA)](**3c**). Selected bond lengths [Å] and angles [°] $^{\#1}$ x, –y+1/2, z: Au(1)–P(1) 2.235(3), Au(1)–S(1) 2.279(3), S(1)–C(5) 1.753(10), P(1)–C(8) 1.849(11), P(1)–C(9) 1.862(9), P(1)–C(9)$^{\#1}$ 1.862(9), P(1)–Au(1)–S(1) 172.50(11), C(5)–S(1)–Au(1) 110.9(4). H are omitted for clarity. (b) View of the packing in the unit cell of complex **3c**.

be similar to the previously described [Au(Spyrimidine)(PTA)].[24] The structure displays a characteristic linear geometry around the gold centre (P1–Au1–S1 of 172.50(11)°). The main difference between the two structures is the disposition of the molecules in the cell. In the previously reported structure, the molecule is associated with an additional unit related by symmetry in a perpendicular rearrangement with Au···Au interactions of 3.3536(7) Å; however the structure of complex **3c** consists of a unique molecule with long intermolecular interactions (Au···Au of 4.154 Å and Au···S of 4.056 Å) in a head-to-tail disposition (Fig. 1b). Another difference is that the Au–P and Au–S distances (2.235(3) and 2.279(3) Å, respectively) are shorter than those described for [Au(Spyrimidine)(PTA)][24] (Au–P 2.2527(18), Au–S 2.3085(18) Å). Longer P–C distances in the PTA phosphane are also observed in **3c** (1.857 Å in average) compared with those found in [Au(Spyrimidine)(PTA)] (1.843 Å on average).

The molecular structure of [Au(SBenzoxazole)(DAPTA)] (**4d**) obtained by X-ray diffraction analysis (Fig. 2) displays a typical linear geometry around the metallic centre with a P1–Au1–S1 angle of 176.72(9)°. To the best of our knowledge this is the first gold DAPTA compound crystallographically characterised, and only examples of palladium,[26,33] platinum,[24] tungsten and chromium[33] derivatives with DAPTA ligands have been described previously. The P–C bond lengths in the DAPTA molecule are approximately 0.129 Å longer than those observed in the free phosphane,[33] however the N(1)–C(13) of 1.365(12) and N(3)–C(15) of 1.377(12) are almost identical compared to its parent. The packing of the individual molecules (Fig. 2b) is influenced by long Au···Au (4.151 Å) and Au···S (3.500 Å) interactions between molecules in a head-to-tail rearrangement, reinforced by intermolecular C–H···N interactions between the DAPTA molecules (C9–H9a···N2^{i} = 2.45 Å, *i* : *1–x*, *y*, *z*; C9···N2 = 3.360(12) Å and angle at H9a of 157°). Additionally, intramolecular C–H···O interactions can be observed in the DAPTA molecule (C9–H9a···O3 = 2.25 Å, C9···O3 = 2.703(11) Å and angle at H9a of 108° and C11–H11a···O2 = 2.29 Å, C11···O2 = 2.723(13) Å and angle at H11a of 106°). The Au–P and Au–S bond lengths of 2.241(2) and 2.316(3) Å, respectively, are in the same range as those observed in gold–PTA[34–37] and gold–PTA thiolate derivatives.[24,38]

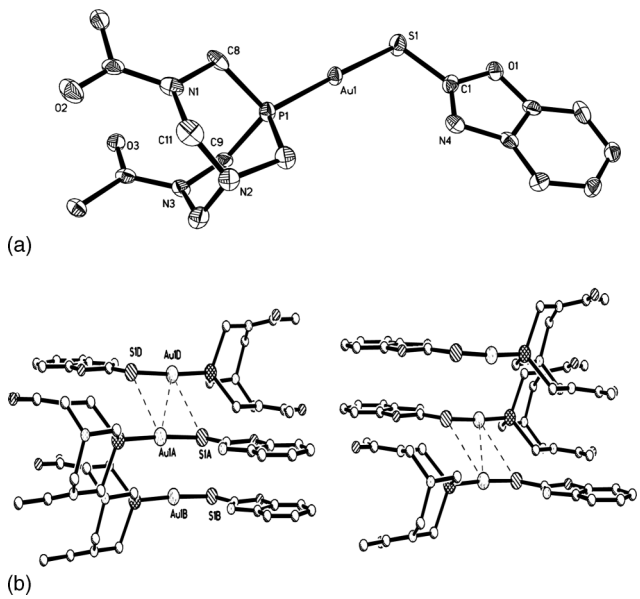

Fig. 2 (a) Molecular structure of [Au(SBenzoxazole)(DAPTA)](**4d**). Selected bond lengths [Å] and angles [°]: Au(1)–P(1) 2.241(2), Au(1)–S(1) 2.316(3), S(1)–C(1) 1.732(10), P(1)–C(9) 1.823(9), P(1)–C(10) 1.832(10), P(1)–C(8) 1.842(10), P(1)–Au(1)–S(1) 176.72(9). H are omitted for clarity. (b) View of the packing in the unit cell of complex **4d**.

Both crystalline structures and the previously reported [Au(Spyrimidine)(PTA)][24] display short interactions between the metallic centres. This fact is very common in thiolate gold(I) derivatives in the solid state. However, in the FAB/MS spectra, only the corresponding molecular peaks are observed and no additional peaks with higher molecular weight are detected, which should be in accordance with the presence of monomers in solution.

The presence of N atoms in the PTA molecule and in some of the thiolate ligands provides the possibility of protonation upon addition of acid. Thus, since such derivatives are water soluble, we have examined sequential protonation of the compounds upon addition of several equivalents of a water solution of HCl (0.05 M) in an aqueous environment, by NMR spectroscopy, at room temperature.

Representative results for [Au(Spyrim)(PTA)](**1c**) are collated in Table 1. As can be observed, the $^{31}P\{^{1}H\}$ NMR signal is shifted to lower field as occurred in PTA complexes with Re[39] and Ru,[40] and it was reported as the decreasing on the net electron-donor character of the protonated PTA. Similarly a deshielding effect was also observed in the ^{1}H NMR, being more pronounced on

Table 1 δ ($^{31}P\{^{1}H\}$ NMR), δ (H^{A}), δ (H^{B}) in $NCH^{A}CH^{B}N$ group and δ (PCH_2N) in ^{1}H NMR after HCl addition to [Au(Spyrim)(PTA)](**1c**) in D_2O

	δ ($NCH^{A}CH^{B}N$)				
HCl Eq.	δ (H^{A})	δ (H^{B})	δ (PCH_2N)	δ (pyrimidine) [J_{HH}/Hz]	δ ($^{31}P\{^{1}H\}$ NMR)
0	4.38	4.46	4.28	7.06(t) [4.8] 8.35(d) [5.1]	–45.4
1	4.39	4.47	4.29	7.07(t) [4.8] 8.36(d) [5.1]	–45.3
2	4.40	4.48	4.30	7.08(t) [4.8] 8.36(d) [5.1]	–44.9
3	4.42	4.49	4.31	7.09(t) [4.8] 8.38(d) [5.1]	–43.6
4	4.44	4.51	4.32	7.10(t) [4.8] 8.39(d) [5.1]	–42.9
5	4.51	4.58	4.34	7.13(t) [4.8] 8.40(d) [5.1]	–42.4

Table 2 Excitation and emission data in the solid state

Compound	298 K		77 K	
	λ_{exc} (nm)	λ_{emis} (nm)	λ_{exc} (nm)	λ_{emis} (nm)
[Au(Spyrim)(PTA)](**1c**)	386	442	389	439
[Au(Spyrim)(DAPTA)](**1d**)	376	438	379	449
[Au(SMe$_2$pyrim)(PTA)](**3c**)	389	450	393	452
[Au(SMe$_2$pyrim)(DAPTA)](**3d**)	335	498	335	497
[Au(SBenzoxazole)(PTA)](**4c**)	360	476	361	473
[Au(SBenzoxazole)(DAPTA)](**4d**)	370	488	372	482
[Au(SGlucosetetracetate)(PTA)](**8c**)	389	450	392	456
[Au(SGlucosetetracetate)(DAPTA)] (**8d**)	396	460	397	462

the NCH^{A}CH^{B}N (an AB system) than on the PCH$_2$N protons, in accordance with a protonation on the N atoms. A small lower field shift was also detected in the corresponding signals of the pyrimidine–thiolate ligand, indicative of the possible protonation of the N atom of the thiolate ligand (Table 1).

Interestingly, some of the thiolate derivatives reported herein display luminescence at room temperature and at 77 K in the solid state (Table 2). As an example, the emission of [Au(SMe$_2$pyrim)(DAPTA)] (**3d**) is plotted in Fig. 3. All the complexes reported in Table 2 emit intensively at 298 and 77 K. The cooling produces small blue shifts (in the range 40–255 cm^{-1}) in the emission of **1c** (155 cm^{-1}), **3d** (40 cm^{-1}), **4c** (133 cm^{-1}) and **4d** (255 cm^{-1}), and red shifts (range 52–293 cm^{-1}) in the emission of **1d** (52 cm^{-1}), **3c** (99 cm^{-1}), **8c** (293 cm^{-1}) and **8d** (94 cm^{-1}). The Stokes shifts observed (> 3500 cm^{-1}) point to a large distortion in the excited state relative to the ground state, consistent with a charge transfer transition. In the case of similar luminescent gold(I) PTA derivatives with substituted benzenethiolate ligands,[41] the emission has been assigned to a metal to ligand charge transfer (LMCT), with the excitation from an orbital associated with the sulfur to the metal-based orbital of the excited state. It is well established that the luminescence found in phosphane thiolate–gold(I) complexes is significantly influenced by the nature of the thiolate,[42] as observed from the data reported in Table 2. In the case of the above mentioned PTA thiolate derivatives,[41] the presence of gold–gold interactions affect the emission maxima, although there is no correlation between such distance and the emission energy, and only sometimes is the emission maximum shifted to lower energies.

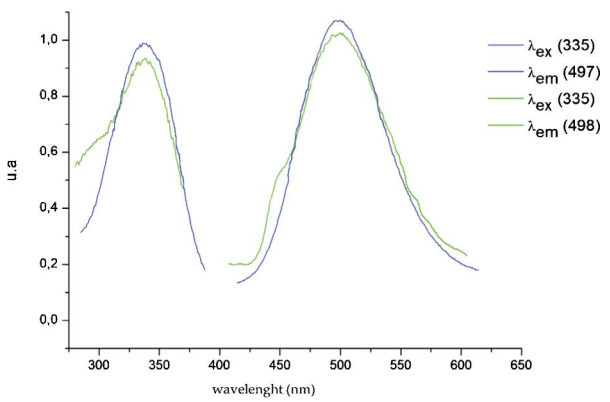

Fig. 3 Excitation and emission spectra of [Au(SMe$_2$pyrim)(DAPTA)](**3d**) at room temperature (green) and at 77 K (blue).

From the analysis of the X-ray structures obtained for **3c** and **4d**, it can be noticed that the gold–gold distances of *ca.* 4.15 Å are relatively long compared to those previously reported for [Au(Spyrimidine)(PTA)][24] (3.3536(7) Å, **1c** in Table 2), while the emission values for the three compounds (**1c**, **3c** and **4d**) are very close to each other and to the rest of the values depicted in Table 2. As a consequence, these results provide support that the observed luminescence originates from the S→Au charge transfer excitation and there is no influence of the gold–gold distances.

The *in vitro* antiproliferative properties of the new Au(I) complexes **1–7(a–b)**, **8c**, and **8d**, as well as those of the already reported PTA and DAPTA derivatives (**1d** and **3–6(c–d)**) were evaluated against the human ovarian cancer cell line (A2780/S) and its cisplatin-resistant variant (A2780/R) in comparison to cisplatin and auranofin. The IC$_{50}$ values (Table 3) were obtained after 72 h drug exposure, using the well established MTT assay (see

Table 3 IC$_{50}$ values of **1–8(a–d)** against ovarian carcinoma cell lines sensitive (A2780/S) or resistant to cisplatin (A2780/R), as compared with cisplatin and auranofin

Compound	IC$_{50}$ (μM)[a]		
	A2780/S	A2780/R	R.F.[b]
[Au(Spyrim)(TPPMS)](**1a**)	117 ± 1	118 ± 1	1.00
[Au(Spyrim)(TPPTS)](**1b**)	12.2 ± 4.2	5.7 ± 1.9	0.46
[Au(Spyrim)(DAPTA)](**1d**)	10.1 ± 1.7	16.1 ± 0.7	1.59
[Au(SMepyrim)(TPPMS)](**2a**)	2.9 ± 0.7	0.6 ± 0.1	0.20
[Au(SMepyrim)(TPPTS)](**2b**)	0.7 ± 0.1	0.4 ± 0.2	0.57
[Au(SMe$_2$pyrim)(TPPMS)](**3a**)	19.8 ± 0.8	16.5 ± 0.6	0.83
[Au(SMe$_2$pyrim)(TPPTS)](**3b**)	2.5 ± 0.2	1.1 ± 0.8	0.44
[Au(SMe$_2$pyrim)(PTA)](**3c**)	0.7 ± 0.3	0.8 ± 0.5	1.14
[Au(SMe$_2$pyrim)(DAPTA)](**3d**)	1.0 ± 0.1	1.2 ± 0.4	1.20
[Au(SBenzoxazole)(TPPMS)](**4a**)	10.5 ± 0.3	6.7 ± 0.2	0.64
[Au(SBenzoxazole)(TPPTS)](**4b**)	34.3 ± 0.3	11.5 ± 0.7	0.34
[Au(SBenzoxazole)(PTA)](**4c**)	2.7 ± 1.1	5.2 ± 2.3	1.92
[Au(SBenzoxazole)(DAPTA)](**4d**)	18.0 ± 0.5	14.9 ± 0.6	0.83
[Au(SBenzothiazol)(TPPMS)](**5a**)	2.4 ± 0.5	1.2 ± 0.5	0.50
[Au(SBenzothiazol)(TPPTS)](**5b**)	2.0 ± 0.5	1.3 ± 0.5	0.65
[Au(SBenzothiazol)(PTA)](**5c**)	0.8 ± 0.2	0.9 ± 0.1	1.12
[Au(SBenzothiazol)(DAPTA)](**5d**)	1.2 ± 0.2	1.1 ± 0.4	0.91
[Au(SBenzoimidazol)(TPPMS)](**6a**)	7.6 ± 0.2	16.4 ± 1.8	3.11
[Au(SBenzoimidazol)(TPPTS)](**6b**)	23.6 ± 2.6	21.4 ± 2.6	0.91
[Au(SBenzoimidazol)(PTA)](**6c**)	8.0 ± 0.6	23.9 ± 2.1	3.0
[Au(SBenzoimidazol)(DAPTA)](**6d**)	0.9 ± 0.3	0.8 ± 0.1	0.88
[Au(SThiazoline)(TPPMS)](**7a**)	10.1 ± 0.8	16.4 ± 0.2	1.63
[Au(SThiazoline)(PTA)](**7c**)	0.7 ± 0.3	1.1 ± 0.1	1.57
[Au(SThiazoline)(DAPTA)](**7d**)	1.1 ± 0.4	0.9 ± 0.1	0.81
[Au(SGlucosetetracetate)(PTA)](**8c**)	10.1 ± 1.8	34.3 ± 1.6	2.98
[Au(SGlucosetetracetate)(DAPTA)](**8d**)	7.5 ± 0.6	27.1 ± 1.2	3.61
cisplatin	4.3 ± 0.5	18.2 ± 1	4.23
auranofin	1.25 ± 0.5	1.5 ± 0.3	1.2

[a] Mean ± SE of at least three determinations. [b] R.F. ratio between IC$_{50}$ values for A2780/R and A2780/S

Experimental for details). Most of the thiolate gold(I) complexes appear to be more cytotoxic than cisplatin and in some cases even of auranofin. Cross-resistance profiles have been evaluated by means of the resistance factor (R.F., see Table 3), which is calculated as the ratio of IC_{50} values between both types of cell lines. In most of the tested derivatives the R.F. values are lower than that calculated for cisplatin, being even 20 times lower in the best case (**2a**). These results support the hypothesis of a different mechanism of action of the gold(I) derivatives with respect to cisplatin. Indeed, none of the reported compounds seem to affect plasmid DNA mobility studied by gel electrophoresis (data not shown), confirming their poor reactivity with nucleic acids.

The antiproliferative properties of the screened compounds seem to depend on both the type of thiolate and phosphane ligands. Among the most effective complexes we observed were those containing the SMepyrim and SMe_2pyrim, as well as Sbenzothiazol and SThiazoline ligands, with IC_{50} values ranging from *ca.* 0.7 to 2.9 μM for the A2780/S cell line, and from 0.4 to 1.3 μM for the resistant cell line. In those cases the phosphane moiety does not appear to have a major effect in modulating the antiproliferative effects. Conversely, for the Spyrim, SBenzoxazole and SBenzoimidazol containing compounds, the phosphane groups can also alter the biological properties, as in the case of compound **1a** (bearing a TPPMS) which is 10 times less effective than the TPPTS and DAPTA analogues **1b** and **1d**, respectively.

Additionally, no correlation between water solubility and cytotoxicity can be inferred. In general, increased water solubility does not correlate with a higher cytotoxic potency or *vice versa*. Complexes with PTA and DAPTA, except the glucosetetraacetate ones, are much less water soluble (values ranging from insoluble to 51 g l^{-1}) than the compounds with the sulphonated phosphanes (values ranging from 85 to 440 g l^{-1}). As an example, the water insoluble derivatives **3c**, **3d**, **5c**, **5d** and **6d** display IC_{50} values as low as **2b**, whose solubility is 340 g l^{-1}, and as **7c** and **7d**, with much more moderate solubility (42 and 51 g l^{-1}, respectively).

In order to evaluate if the cell uptake of the compounds might affect their cytotoxic properties, cell extracts from A2780/S and A2780/R cancer cells treated with 1 μM of metal compound for 3 h at 37 °C were analyzed by ICP-MS, as described in the Experimental section. The obtained results for representative compounds expressed as pmol Au/10^6 cells are reported in Table 4. Remarkably, the uptake of the poorly cytotoxic compound **1a** (IC_{50} *ca.* 100 μM) is *ca.* 3–4 times lower than in the case of the active analogue **1b** in each cell line, and about 10 fold less efficient than in the case of auranofin, a fact that may account for the difference in cytotoxic potency between the compounds. Indeed, auranofin has the best cell uptake among the investigated Au(I) complexes in both cell lines, corresponding to its higher cytotoxic effect.

Table 4 Cell uptake of Au(I) phosphane complexes in A2780/S and A2780/R cancer cell lines after treatment with 1 μM metal compound for 3 h

	pmol Au/10^6 cells[a]	
Compound	A2780/S	A2780/R
1a [Au(Spyrim)(TPPMS)]	288 ± 93	393 ± 102
1b [Au(Spyrim)(TPPTS)]	806 ± 91	941 ± 140
8c [Au(SGlucosetetracetate)(PTA)]	925 ± 244	1102 ± 259
8d [Au(SGlucosetetracetate)(DAPTA)]	2587 ± 522	1886 ± 189
auranofin	2946 ± 603	4638 ± 1234

[a] Mean ± SE of at least three determinations.

Interestingly, the gold cell uptake for the thioglucose derivatives **8c** and **8d** seems not to account for the differences in the cytotoxic potency of the two compounds towards both cancer cell lines. In fact, the higher IC_{50} values of the two complexes for the cisplatin resistant variant do not correspond to a lower Au uptake with respect to the one recorded on the A2780/S cell line. Moreover, the thioglucose analogues having similar IC_{50} values in the case of the A2780/S cells do not manifest comparable cell uptake properties in the same cell line (**8c** has a 2-3-fold reduced uptake relatively to **8d**). It is worth mentioning that application of carbohydrate–metal complexes is an example of a targeted approach exploiting the biochemical and metabolic functions of diverse sugars in living organisms for transport and accumulation.[27] Natural carbohydrates and synthetic derivatives possess a manifold of donors endowing them with the ability to coordinate metal centers and providing some additional advantages over other ligands, *e.g.*, biocompatibility, non-toxicity, enantiomeric purity, water solubility, and well-explored chemistry. Indeed, compounds **8c**–**8d** might exploit different cell uptake mechanisms, with respect to the other complexes in the series, involving glucose transporters, and therefore manifesting more complex cellular responses.

Conclusions

In this study, water soluble thiolate Au(I) complexes with phosphane ligands, namely TPPMS, TPPTS, PTA and DAPTA, were synthesized and characterized for their chemical/structural properties. Interestingly, the compounds present luminescence properties in the solid state, which seems to be due to S→Au charge transfer excitations. Addition of acid to a water solution of some of the PTA thiolate derivatives reveals a decrease in the nucleophilic character of the phosphane as result of its N-atom protonation.

The compounds were also tested for their antiproliferative activities on human ovarian cancer cell lines A2780/S and A2780/R and resulted to exert a wide range of cytotoxic activities, mainly in the low μM range. Among the best antiproliferative agents, those containing SMepyrim and SMe_2pyrim, as well as Sbenzothiazol and SThiazoline ligands, reached the lowest IC_{50} values, in some cases better than the reference drugs cisplatin and auranofin. ICP-MS analysis of cell extracts out of A2780 cells pre-treated with gold compounds, including auranofin, demonstrated that the cytotoxicity is proportional to the gold uptake. However, in the case of the thioglucose derivatives, the strongest antiproliferative effects do not correspond to higher values of intracellular gold concentration. In the latter case, the observed uptake might be influenced by the affinity for the thioglucose moiety with the sugar receptors of the cancer cells, therefore the sugar-based gold(I) complexes manifest more complex correlations between cytotoxicity and cell uptake with respect to the other phosphane derivatives.

Experimental

General

NMR spectra were recorded on 400 MHz Bruker Avance spectrometer. Chemical shifts are quoted relative to external TMS

(^{1}H) or 85% H_3PO_4 (^{31}P); coupling constants are reported in Hz. FAB mass spectra were measured on a Micromass Autospec spectrometer in positive ion mode using NBA as matrix. IR spectra were recorded as KBr or polyethylene disks on a Nicolet Impact 410 or JASCO FTIR (far-IR) spectrometers. Steady-state photoluminescence spectra were recorded with a Jobin–Yvon–Horiba fluorolog FL-3-11 spectrometer using band pathways of 3 nm for both excitation and emission. Elemental analyses were obtained in-house using a LECO CHNS-932 microanalyser. The phosphanes PTA[43] DAPTA,[26,33] TPPMS,[44] and [AuCl(PR′$_3$)][26,30] were prepared according to published methods. A sample of TPPTS was kindly provided by European Oxo GmbH. Cisplatin was purchased from Sigma–Aldrich and auranofin from Alexis Biochemicals.

Synthesis of the [Au(SR)(PR′$_3$)] complexes

To a solution of KOH (0.022 g, 0.385 mmol) in MeOH (*ca.* 10 mL) containing the thiol compound (0.308 mmol) was added [AuCl(PR′$_3$)] (PR′$_3$ = TPPMS, TPPTS) (0.257 mmol). After stirring the mixture for *ca.* 20 h at room temperature the solutions were evaporated to dryness under vacuum and the residue extracted in dichloromethane (3 × 10 mL). The combined extracts were passed through Celite and concentrated under vacuum to *ca.* 5 mL. Addition of pentane or Et_2O precipitated the products, which were isolated by filtration and dried in air.

Using this method the following complexes were prepared:

[Au(Spyrim)(TPPMS)](1a). 49% yield, pale yellow solid. ^{1}H NMR (400 MHz, $CDCl_3$, 25 °C): δ = 7.01 (t, J = 4.8 Hz, 1H, pyrim-H^5), 7.38–7.65 (m, 12H, *o*-, *m*- y *p*-Ph, *o*-$PhSO_3Na$ (H^6), *m*-$PhSO_3Na$), 7.91–8.10 (m, 2H, *o*-$PhSO_3Na$ (H_2), *p*-$PhSO_3Na$), 8.32 (d, J = 5.1 Hz, 2H, pyrim-H^4, H^6) ppm. ^{31}P{^{1}H} NMR (162 MHz, $CDCl_3$, 25 °C): δ = 37.1 ppm. FAB MS: m/z 673 $[M]^+$; elemental analysis calcd. (%) for $C_{22}H_{17}AuN_2NaO_3PS_2$ (672.44): C 39.29, H 2.55, N 4.17; found: C 39.01, H 2.03, N 4.01. S_{20}°,H_2O: 90 g L^{-1}

[Au(Spyrim)(TPPTS)](1b). 72% yield, pale yellow solid. ^{1}H NMR (400 MHz, D_2O, 25 °C): δ = 6.89 (t, J = 4.8 Hz, 1H, pyrim-H^5) 7.46–7.65 (m, 6H, *o*-$PhSO_3Na$ (H^6), *m*-$PhSO_3Na$), 7.74–7.83 (*m*, 6H, *o*-$PhSO_3Na$ (H^2), *p*-$PhSO_3Na$), 8.22 (d, J = 5.1 Hz, 2H, pyrim-H^4, H^6) ppm. ^{31}P{^{1}H} NMR (162 MHz, D_2O, 25 °C): δ = 36.7 ppm. FAB MS: m/z 877 $[M]^+$; elemental analysis calcd. (%) for $C_{22}H_{15}AuN_2Na_3O_9PS_4$ (876.53): C 30.15, H 1.72, N 3.20; found: C 30.65, H 1.54, N 2.69. S_{20}°, H_2O: 102 g L^{-1}

[Au(SMepyrim)(TPPMS)](2a). 63% yield, pale yellow solid. ^{1}H NMR (400 MHz, MeOD, 25 °C): δ = 2.54 (s, 3H, CH_3), 7.21 (d, J = 5.3 Hz, 1H, pyrim-H^5), 7.49–7.62 (m, 14H, *o*-, *m*- y *p*-Ph, *o*-$PhSO_3Na$ (H^6), *m*-$PhSO_3Na$, *o*-$PhSO_3Na$ (H^2), *p*-$PhSO_3Na$), 8.29 (d, J = 5.0 Hz, 1H, pyrim-H^6). ^{31}P{^{1}H} NMR (162 MHz, MeOD, 25 °C): δ = 36.1 ppm. FAB MS: m/z 687 $[M]^+$; elemental analysis calcd. (%) for $C_{23}H_{19}AuN_2NaO_3PS_2$ (686.47): C 40.24, H 2.79, N 4.08; found: C 39.71, H 3.50, N 3.92. S_{20}°,H_2O: 85g L^{-1}

[Au(SMepyrim)(TPPTS)](2b). 56% yield, pale yellow solid. ^{1}H NMR (400 MHz, MeOD, 25 °C): δ = 2.34 (s, 3H, CH_3), 7.05 (d, J = 5.2 Hz, 1H, pyrim-H^5), 7.36–7.52 (m, 6H, *o*-$PhSO_3Na$ (H^6), *m*-$PhSO_3Na$), 7.72–7.80 (*m*, 6H, *o*-$PhSO_3Na$ (H^2), *p*-$PhSO_3Na$), 8.25 (d, J = 5.1 Hz, 1H, pyrim-H^6). ^{31}P{^{1}H} NMR (162 MHz, MeOD, 25 °C): δ = 36.3 ppm. FAB MS: m/z 890 $[M]^+$; elemental analysis calcd. (%) for $C_{23}H_{17}AuN_2Na_3O_9PS_4$ (890.56): C 31.02, H 1.92, N 3.15; found: C 31.21, H 1.78, N 2.90. S_{20}°,H_2O: 344 g L^{-1}

[Au(SMe$_2$pyrim)(TPPMS)] (3a). 58% yield, pale yellow solid. ^{1}H NMR (400 MHz, MeOD, 25 °C): δ = 2.24 (s, 6H, CH_3), 6.57 (s, 1H, pyrim-H^4), 7.43–7.65 (m, 12H, *o*-, *m*- y *p*-Ph, *o*-$PhSO_3Na$ (H^6), *m*-$PhSO_3Na$), 7,90–8,09 (m, 2H, *o*-$PhSO_3Na$ (H^2), *p*-$PhSO_3Na$). ^{31}P{^{1}H} NMR (162 MHz, MeOD, 25 °C): δ = 36.1 ppm. FAB MS: m/z 701 $[M]^+$; elemental analysis calcd. (%) for $C_{24}H_{21}AuN_2NaO_3PS_2$ (700.5): C 41.15, H 3.02, N 4.00; found: C 40.96, H 2.93, N 3.68. S_{20}°,H_2O: 212 g L^{-1}

[Au(SMe$_2$pyrim)(TPPTS)] (3b). 89% yield, yellow solid. ^{1}H NMR (400 MHz, D_2O, 25 °C): δ = 2.19 (s, 6H, CH_3), 6.62 (s, 1H, pyrim-H^4), 7.50–7.74 (m, 6H, *o*-$PhSO_3Na$ (H^6), *m*-$PhSO_3Na$), 7.77–7.92 (*m*, 6H, *o*-$PhSO_3Na$ (H^2), *p*-$PhSO_3Na$) ppm. ^{31}P{^{1}H} NMR (162 MHz, D_2O, 25 °C): δ = 36.2 ppm. FAB MS: m/z 905 $[M]^+$; elemental analysis calcd. (%) for $C_{24}H_{19}AuN_2Na_3O_9PS_4$ (904.59): C 31.87, H 2.12, N 3.10; found: C 31.38, H 2.32, N 2.72. S_{20}°,H_2O: 480 g L^{-1}

[Au(Sbenzoxazole)(TPPMS)] (4a). 69% yield, yellow solid. ^{1}H NMR (400 MHz, D_2O, 25 °C): δ = 7.08–7.17 (m, 2H, benzoxazol-H^2, HH^3), 7.27–7.34 (m, 2H, benzoxazol-H^1, HH^4), 7.47–7.93 (m, 12H, *o*-, *m*- y *p*-Ph, *o*-$PhSO_3Na$ (H^6), *m*-$PhSO_3Na$), 7.93–8.10 (m, 2H, *o*-$PhSO_3Na$ (H^2), *p*-$PhSO_3Na$). ^{31}P{^{1}H} NMR (162 MHz, D_2O, 25 °C): δ = 36.7 ppm. FAB MS: m/z 713 $[M]^+$; elemental analysis calcd. (%) for $C_{25}H_{18}AuNNaO_4PS_2$ (711.47): C 31.87, H 2.12, N 3.10; found: C 41.87, H 2.01, N 1.54. S_{20}°,H_2O: 90 g L^{-1}

[Au(Sbenzoxazole)(TPPTS)] (4b). 85% yield, yellow solid. ^{1}H NMR (400 MHz, D_2O, 25 °C): δ = 7.01–7.06 (m, 2H, benzoxazol-H^2, H^3), 7.11–7.26 (m, 2H, benzoxazol-H^1, HH^4), 7.36–7.52 (m, 6H, *o*-$PhSO_3Na$ (H^6), *m*-$PhSO_3Na$), 7.47–7.92 (*m*, 6H, *o*-$PhSO_3Na$ (H^2), *p*-$PhSO_3Na$). ^{31}P{^{1}H} NMR (162 MHz, D_2O, 25 °C): δ = 36.6 ppm. FAB MS: m/z 917 $[M]^+$; elemental analysis calcd. (%) for $C_{25}H_{16}AuNNa_3O_{10}PS_4$ (915.56): C 32.80, H 1.76, N 1.53; found: C 31.86, H 1.53, N 1.26. S_{20}°,H_2O: 325 g L^{-1}

[Au(Sbenzothiazole)(TPPMS)] (5a). 68% yield, yellow solid. ^{1}H NMR (400 MHz, D_2O, 25 °C): δ = 7.20 (dt, J = 7.1/1.3Hz, 1H, benzothiaz-H^3), 7.33 (dt, J = 7.1/1.3Hz, 1H, benzothiaz-H^2), 7.45–7.70 (m, 13H, *o*-, *m*- y *p*-Ph, *o*-$PhSO_3Na$ (H^6), *m*-$PhSO_3Na$, benzothiaz-H^4), 7.73–8.10 (m, 3H, *o*-$PhSO_3Na$ (H^2), *p*-$PhSO_3Na$, benzothiaz-H^1) ppm. ^{31}P{^{1}H} NMR (162 MHz, D_2O, 25 °C): δ = 36.7 ppm. FAB MS: m/z 728 $[M]^+$; elemental analysis calcd. (%) for $C_{25}H_{18}AuNNaO_3PS_3$ (727.54): C 41.27, H 2.49, N 1.93; found: C 41.06, H 2.26, N 1.72. S_{20}°,H_2O: 110 g L^{-1}

[Au(Sbenzothiazole)(TPPTS)] (5b). 74% yield, yellow solid. ^{1}H NMR (400 MHz, D_2O, 25 °C): δ = 7.19–7.29 (m, 2H, benzothiaz-H^3, HH^2), 7.47–7.75 (m, 7H, *o*-$PhSO_3Na$ (H^6), *m*-$PhSO_3Na$, benzothiaz-H^4), 7.78–7.94 (*m*, 6H, *o*-$PhSO_3Na$ (H^2), *p*-$PhSO_3Na$, benzothiaz-H^1). ^{31}P{^{1}H} NMR (162 MHz, D_2O, 25 °C): δ = 36.7 ppm. FAB MS: m/z 936 $[M]^+$; elemental analysis calcd. (%) for $C_{25}H_{16}AuNNa_3O_9PS_5$ (931.63): $C_{25}H_{16}AuNNa_3O_9PS_5$ (931.63); found: C 32.50, H 1.75, N 2.03. S_{20}°,H_2O: 440 g L^{-1}

[Au(Sbenzimidazole)(TPPMS)] (6a). 60% yield, pale yellow solid. ^{1}H NMR (400 MHz, D_2O, 25 °C): δ = 7.02–7.13 (m, 2H,

benzimidaz-H^2, H^3), 7.18–7.33 (m, 2H, benzimidaz-H^1, H^4), 7.45–7.70 (m, 12H, *o*-, *m*- y *p*-Ph, *o*-$PhSO_3Na$ (H^6), *m*-$PhSO_3Na$), 7.93–8.10 (m, 2H, *o*-$PhSO_3Na$ (H^2), *p*-$PhSO_3Na$), 11.96 (s, 1H, N*H*). $^{31}P\{^1H\}$ NMR (162 MHz, D_2O, 25 °C): δ = 37.3 ppm. FAB MS: *m*/*z* 712 $[M]^+$; elemental analysis calcd. (%) for $C_{25}H_{19}AuN_2NaO_3PS_2$ (710.49): C 42.26, H 2.70, N 3.94; found: C 41.89, H 2.88, N 3.72. $S_{20}°$,H_2O: 101 g L^{-1}

[Au(Sbenzimidazole)(TPPTS)] (6b). 85% yield, yellow solid. ^1H NMR (400 MHz, D_2O, 25 °C): δ = 7.07–7.19 (m, 2H, benzimidaz-H^3, H^2), 7.24–7.36 (m, 2H, benzimidaz-H^1, H^4), 7.39–7.52 (m, 6H, *o*-$PhSO_3Na$ (H^6), *m*-$PhSO_3Na$), 7.72–7.80 (*m*, 6H, *o*-$PhSO_3Na$ (H^2), *p*-$PhSO_3Na$), 12.20 (br. s, 1H, N*H*). $^{31}P\{^1H\}$ NMR (162 MHz, D_2O, 25 °C): δ = 37.6 ppm. FAB MS: *m*/*z* 916 $[M]^+$; elemental analysis calcd. (%) for $C_{25}H_{17}AuN_2Na_3O_9PS_4$ (914.58): C 32.83, H 1.87, N 3.06; found: C 33.42, H 1.70, N 2.75. $S_{20}°$,H_2O: 250 g L^{-1}

[Au(Sthiazoline)(TPPMS)] (7a). 65% yield, yellow solid. ^1H NMR (400 MHz, D_2O, 25 °C): δ = 3.42 (t, *J* = 7.8 Hz, 2H, thiazoline), 4.11 (t, *J* = 8.0 Hz, 2H, thiazoline) 7.35–7.64 (m, 12H, *o*-Ph, *m*-Ph, *p*-Ph, *o*-$PhSO_3Na$ (H^6), *m*-$PhSO_3Na$), 7.87–8.02 (*m*, 2H, *o*-$PhSO_3Na$ (H^2), *p*-$PhSO_3Na$) ppm. $^{31}P\{^1H\}$ NMR (162 MHz, D_2O, 25 °C) δ = 36.7 ppm. FAB MS: *m*/*z* 678 $[M]^+$; elemental analysis calcd. (%) for $C_{21}H_{16}AuNNaO_3PS_3$ (679.50): C 37.12, H 2.06, N 2.06; found: C 36.98, H 2.32, N 1.78. $S_{20}°$,H_2O: 99 g L^{-1}

Synthesis of [Au(Sglucosetetraacetate)(PR′$_3$)] (PR′$_3$ = PTA (8a) and DAPTA (8b)) complexes

A mixture of [AuCl(PR′$_3$)] (0.26 mmol), 1-thio-β-D-glucose tetraacetate (0.26 mmol) and K_2CO_3 (0.28 mmol) in EtOH (10 mL) and water (10 mL) was stirred for *ca.* 18 h. The solvents were removed under reduced pressure, and the solid residue was extracted with acetone and filtered through Celite. The addition of diethylether to the filtrate afforded the colourless product, which was isolated by filtration and dried in air.

8a. Yield: 79%, colourless solid. ^1H NMR (400 MHz, dmso-d^6, 25 °C): δ = 1.90, 1.97, 1.99, 2.03 (s, 3H, Me), 3.88 (ddd, *J* = 9.8/4.5/2.3Hz, 1H, H^5), 3.97 (dd, *J* = 12.4/2.4Hz, 1H, CH_2), 4.09 (dd, *J* = 12.1/4.5Hz, 1H, CH_2), 4.30 (s, 6H, NCH_2P), 4.34, 4.53 (J_{AB} = 12.8 Hz, 6H, NCH_2N), 4.62 (t, *J* = 9.3 Hz, 1H, H^2), 4.85 (t, *J* = 9.9 Hz, 1H, H^4), 5.11 (t, 2H, *J* = 9.6 Hz, H^1, H^3) ppm. $^{31}P\{^1H\}$ NMR (162 MHz, dmso-d^6, 25 °C): δ = –47.0 ppm. $C_{20}H_{31}AuN_3O_9PS$ (717.48): calcd. C 33.48, H 4.35, N 5.86, found C 33.34, H 4.25, N 6.09. $S_{20}°$, H_2O: 220 g L^{-1}

8b. Yield: 79%, colourless solid. ^1H NMR (400 MHz, D_2O, 25 °C): δ = 1.95, 1.98, 2.02, 2.05 (s, 3 H, Me), 2.06 (s, 6H, CO*Me*), 3.84 (dt, *J* = 15.6/3.9 Hz, 1 H, H^5), 3.95–4.00 (m, 2 H, NCH_2P), 4.03 (s, 1 H, NCH_2P), 4.11 (dd, *J* = 12.4, 1.6 Hz, 1 H, CH_2), 4.2 (d, 1 H, *J* = 14.4 Hz, NCH_2N), 4.30 (dd, *J* = 12.8/3.6 Hz, 1 H, CH_2), 4.30–4.38 (m, 1 H, NCH_2P), 4.80 (d, *J* = 10 Hz, 1 H, NCH_2N), 4.84 (t, *J* = 9.2 Hz, 1 H, H^2), 5.01 (d, *J* = 5.6 Hz, 1 H, NCH_2P), 5.04 (t, *J* = 10 Hz, 1 H, H^4), 5.15 (t, *J* = 9.2 Hz, 2 H, H^1H^3), 5.20 (d, *J* = 9.2 Hz, 1H, NCH_2N), 5.36 (dd, *J* = 16/8.4 Hz, 1 H, NCH_2P), 5.54 (d, *J* = 14 Hz, 1H, NCH_2N) ppm. $^{31}P\{^1H\}$ NMR (162 MHz, D_2O, 25 °C): δ = –22.3 ppm. $C_{23}H_{35}AuN_3O_{11}PS$ (789.54): calcd. C 34.99, H 4.47, N 5.32; found C 34.87, H 4.36, N 5.03. $S_{20}°$, H_2O: 220 g L^{-1}

Table 5 Crystal Data and Data Collection and Refinement for complexes [Au(SMe_2Pyrim)(PTA)] (**3c**) and [Au(SBenzoxazole)(DAPTA)] (**4d**)

	3c	**4d**
Empirical formula	$C_{12}H_{19}AuN_5PS$	$C_{16}H_{22}AuN_4O_4PS$
Mol wt	493.32	594.37
Color, habit	Colourless, needle	Colourless, plate
Space group	Monoclinic, $P2_1/m$	Triclinic, $P\bar{1}$
a (Å)	10.735(5)	6.0539(10)
b (Å)	7.029(5)	10.5087(18)
c (Å)	13.608(5)	15.828(3)
α (°)	90	97.007(3)°
β (°)	109.139(5)	96.101(3)
γ (°)	90	98.188(3)
V(Å^3)	970.1(9)	981.4(3)
Z	2	2
D(calc) (g cm^{-3})	1.689	2.005
μ (mm^{-1})	7.771	7.713
θ Range (deg)	3.15 to 25.00	1.98 to 24.50
N. data collected	15722	9236
N. unique data	1846 [*R*(int) = 0.0876]	3245 [*R*(int) = 0.0430]
$R_1{}^a(F^2 > 2\sigma(F^2))$	0.0369	0.0423
$\varpi R_2{}^b$(all data)	0.0832	0.1111
S^c (all data)	0.970	1.055

^{a} $R_1(F) = \sum\|F_o\| - |F_c\|/\sum |F_o|$. ^{b} $\varpi R_2(F^2) = [\sum[\varpi(F_o^2 - F_c^2)^2]/\sum[w(F_o^2)^2]]^{1/2}$, $w^{-1} = [\sigma^2(F_o^2)+(\alpha P)^2+bP]$, where $P = [\max(F_o^2, 0)+2F_c^2)]/3$. ^{c} $S = [\sum[\varpi(F_o^2 - F_c^2)^2]/(n-p)]^{1/2}$, where *n* is the number of reflections and *p* the number of refined parameters.

X-ray diffraction analysis

Crystals suitable for X-ray diffraction were obtained by slow diffusion of diethyl ether into ethanolic solutions. A summary of the fundamental crystal and refinement data of compounds [Au(SMe_2pyrimidine)(PTA)] (**3c**) and [Au(SBenzoxazole)(DAPTA)] (**4d**) is given in Table 5. The crystals were mounted on glass fiber with inert oil and centred in a Bruker-Smart CCD diffractometer with graphite-monochromated Mo-Kα (λ = 0.7107 Å) radiation for data collection. The diffraction frames were integrated by using the SAINT[45] package and corrected for absorption with SADABS.[46] The structure of **3c** was solved by direct methods using SHELXS[47] and **4d** by sir2002.[48] Full-matrix least squares refinement was carried out using SHELXL minimizing $\omega(F_0{}^2{}^*-F_c{}^2)^2$. Hydrogen atoms were included by using a riding model. In the case of **4d** the hydrogens of water molecules were not located. Weighted *R* factors (R_w) and all goodness of fit *S* values are based on F^2; conventional R factors (*R*) are based on *F*. The PLATON SQUEEZE[49,50] algorithm was applied to **3c** to model the diffuse contribution from a highly disordered solvent of crystallisation to the electron density. The complete crystallographic data have also been deposited with the Cambridge Crystallographic Data Centre [Deposition numbers are CCDC 790251 and 790252 for compounds **3c** and **4d** respectively, see ESI†].

Antiproliferative assays

Human A27807S and A2780/R cells were obtained from the European Centre of Cell Cultures (ECACC, Salisbury, UK). All cell culture reagents were obtained from Gibco-BRL (Basel, Switzerland). Cells were grown in RPMI 1640 medium containing 10% fetal calf serum (FCS) and antibiotics. Stock solutions of the complexes (in DMSO) were diluted in complete medium to the

required concentration. DMSO at comparable concentrations did not show any effects on cell cytotoxicity.

For cytotoxicity screening, cells were grown in 96-well cell culture plates (Corning, NY) at a density of 25×10^3 cells per well. The culture medium was replaced with fresh medium containing the complexes at concentrations varying from 0 to 20 μM, with an exposure time of 72 h. Thereafter, the medium was replaced by fresh medium and cell survival was measured using the MTT test as previously described. Briefly, 3-(4,5-dimethyl-2-thiazoyl)-2,5-diphenyltetrazolium bromide (MTT, Merck) was added at 250 μg mL^{-1} and incubation was continued for 2 h. Then the cell culture supernatants were removed, the cell layer was dissolved in DMSO, and absorbance at 540 nm was measured in a 96-well multiwell-plate reader (iEMS Reader MF, Labsystems, Bioconcept, Switzerland) and compared to the values of control cells incubated in the absence of complexes. Experiments were conducted in quadruplicate wells and repeated at least twice.

Cell uptake studies and ICP-MS analysis

For evaluation of the cell uptake, cells were seeded in 6-well plates and grown to approximately 70% confluency and incubated with the corresponding metallodrug at 1 μM for 3 h. At the end of the incubation period, cells were rinsed cells with 5 mL of PBS, detached by adding 0.4 mL enzyme free cell dissociation solution (Millipore, Switzerland) and collected by centrifugation. Cell lysis was achieved using a freeze-thaw technique that was recently found to be suitable for cell uptake studies.[51] All samples were analyzed for their protein content (to establish the number of cells per sample) prior to ICP-MS determination using a BCA assay (Sigma Aldrich, Switzerland). All samples were digested in ICP-MS grade concentrated hydrochloric acid (Sigma Aldrich, Switzerland) for 3 h at room temperature and filled to a total volume of 8 ml with ultrapure water. Indium was added as an internal standard at a concentration of 0.5 ppb. Determinations of total metal contents were achieved on an Elan DRC II ICP-MS instrument (Perkin Elmer, Switzerland) equipped with a Meinhard nebulizer and a cyclonic spray chamber. The ICP-MS instrument was tuned daily using a solution provided by the manufacturer containing 1 ppb each of Mg, In, Ce, Ba, Pb and U. External standards were prepared gravimetrically in an identical matrix to the samples (with regard to internal standard and hydrochloric acid) with single element standards obtained from CPI International (Amsterdam, The Netherlands).

Acknowledgements

We thank the Ministerio de Ciencia e Innovación (CTQ2008-06716-CO3-01) for financial support. The authors wish also to thank COST D39 action for stimulating discussion. AC thanks the Swiss National Science Foundation (AMBIZIONE project no. PZ00P2-121933) and the Swiss Confederation (Action COST D39 - Accord de recherche - SER project no. C09.0027) for financial support.

References

1 C. F. Shaw, *Chem. Rev.*, 1999, **99**, 2589.
2 D. A. Gordon, *Textbook of rheumatology*, 4th edn, W. N. Kelly, E. D. Harris, S. Ruddy and S. B. Sledge, editors, Philadelphia, W. B. Saunders Company, 1989.
3 W. F. Kean and I. R. L. Kean, *Inflammopharmacology*, 2008, **16**, 112.
4 E. R. T. Tieknik, *Inflammopharmacology*, 2008, **16**, 138.
5 I. Kostova, *Anti-Cancer Agents Med. Chem.*, 2006, **6**, 19.
6 E. R. T. Tiekink, *Crit. Rev. Oncol. Hematol.*, 2002, **42**, 225.
7 L. Messori and G. Marcon, *Metal Ions in Biological Systems. Gold Complexes as antitumour agents*, A Sigel and H Sigel (Eds), Marcel Dekker Inc, New York, 2004.
8 A. Casini, C. Hartinger, C. Gabbiani, E. Mini, P. J. Dyson, B. K. Keppler and L. Messori, *J. Inorg. Biochem.*, 2008, **102**, 564.
9 S. Nobili, E. Mini, I. Landini, C. Gabbiani, A. Casini and L. Messori, *Med. Res. Rev.*, 2010, **30**, 550.
10 L. Ronconi and D. Fregona, *Dalton Trans.*, 2009, 10670.
11 R. W. Y. Sun and C. M. Che, *Coord. Chem. Rev.*, 2009, **253**, 1682.
12 A. Bindoli, M. P. Rigobello, G. Scutari, C. Cabbiani, A. Casini and L. Mesori, *Coord. Chem. Rev.*, 2009, **253**, 1692.
13 I. Ott, *Coord. Chem. Rev.*, 2009, **253**, 1670.
14 A. Casini, C. Hartinger, C. Gabbiani, E. Mini, P. J. Dyson, B. K. Keppler and L. Messori, *J. Inorg. Biochem.*, 2008, **102**, 564.
15 K. M. Hindi, M. J. Panzner, C. A. Tessier, C. L. Cannon and W. J. Youngs, *Chem. Rev.*, 2009, **109**, 3859.
16 M. J. McKeage, L. Maharaj and S. J. Berners-Price, *Coord. Chem. Rev.*, 2002, **232**, 127.
17 P. J. Barnard and S. J. Berners-Price, *Coord. Chem. Rev.*, 2007, **251**, 1889.
18 K. P. Bhabak, B. J. Bhuyan and G. Mugesh, *Dalton Trans.*, 2011, 2099.
19 X. Zhang, M. Frezza, V. Milacic, L. Ronconi, Y. H. Fan, C. F. Bi, D. Fregona and Q. P. Dou, *J. Cell. Biochem.*, 2010, **109**, 162.
20 A. Casini, G. Kelter, C. Gabbiani, M. A. Cinellu, G. Minghetti, D. Fregona, H. H. Fiebig and L. Messori, *JBIC, J. Biol. Inorg. Chem.*, 2009, **14**, 1139.
21 M. V. Baker, P. J. Barnard, S. J. Berners-Price, S. K. Brayshaw, J. L. Hickey, B. W. Skelton and A. H. White, *Dalton Trans.*, 2006, 3708.
22 F. Mendes, M. Groessl, A. A. Nazarov, Y. O. Tsybin, G. Sava, I. Santos, P. J. Dyson and A. Casini, *J. Med. Chem.*, 2011, **54**, 2196.
23 F. Magherini, A. Modesti, L. Bini, M. Puglia, I. Landini, S. Nobili, E. Mini, M. A. Cinellu, C. Gabbiani and L. Messori, *JBIC, J. Biol. Inorg. Chem.*, 2010, **15**, 573.
24 S. Miranda, E. Vergara, F. Mohr, D. de Vos, E. Cerrada, A. Mendia and M. Laguna, *Inorg. Chem.*, 2008, **47**, 5641.
25 E. Vergara, A. Casini, F. Sorrentino, O. Zava, E. Cerrada, M. P. Rigobello, A. Bindoli, M. Laguna and P. J. Dyson, *ChemMedChem*, 2010, **5**, 96.
26 E. Vergara, S. Miranda, F. Mohr, E. Cerrada, E. R. T. Tiekink, P. Romero, A. Mendia and M. Laguna, *Eur. J. Inorg. Chem.*, 2007, 2926.
27 C. G. Hartinger, A. A. Nazarov, S. M. Ashraf, P. J. Dyson and B. K. Keppler, *Curr. Med. Chem.*, 2008, **15**, 2574.
28 M. M. Welling and R. Alberto, *Nucl. Med. Commun.*, 2010, **31**, 239.
29 L. A. Jones, S. Sanz and M. Laguna, *Catal. Today*, 2007, **122**, 403.
30 S. Sanz, L. A. Jones, F. Mohr and M. Laguna, *Organometallics*, 2007, **26**, 952.
31 S. Sanz, *PhD thesis*, Zaragoza, 2007.
32 B. T. Elie, C. Levine, I. Ubarretxena-Belandia, A. Varela-Ramirez, R. J. Aguilera, R. Ovalle and M. Contel, *Eur. J. Inorg. Chem.*, 2009, 3421.
33 D. J. Darensbourg, C. G. Ortiz and J. W. Kamplain, *Organometallics*, 2004, **23**, 1747.
34 Z. Assefa, B. G. McBurnett, R. J. Staples and J. P. j. Fackler, *Inorg. Chem.*, 1995, **34**, 4965.
35 Z. Assefa, R. J. Staples and J. P. j. Fackler, *Acta Crystallogr., Sect. C: Cryst. Struct. Commun.*, 1996, **52**, 305.
36 F. Mohr, S. Sanz, E. R. T. Tieknik and M. Laguna, *Organometallics*, 2006, **25**, 3084.
37 F. Mohr, E. Cerrada and M. Laguna, *Organometallics*, 2006, **25**, 644.
38 J. M. Forward, D. Bohmann, J. P. j. Fackler and R. J. Staples, *Inorg. Chem.*, 1995, **34**, 6330.
39 P. Smolenski and A. J. L. Pombeiro, *Dalton Trans.*, 2008, 87.
40 C. A. Mebi and B. J. Frost, *Organometallics*, 2005, **24**, 2339.
41 J. M. Forward, D. Bohmann, J. P. Fackler and R. J. Staples, *Inorg. Chem.*, 1995, **34**, 6330.
42 E. R. T. Tiekink and J.-G. Kang, *Coord. Chem. Rev.*, 2009, **253**, 1627.
43 D. J. Daigle, *Inorg. Synth.*, 1998, **32**, 40.
44 F. Joó, J. Kovács, A. Kathó, A. C. Bényei, T. Decuir and D. J. Darensbourg, *Inorg. Synth.*, 1998, **32**, 1.

45 X. de Leval, M. Ilies, A. Casini, J. M. Dogne, A. Scozzafava, E. Masini, F. Mincione, M. Starnotti and C. T. Supuran, *J. Med. Chem.*, 2004, **47**, 2796.
46 G. M. Sheldrick, 1996, *SADABS Empirical absorption program*, University of Göttingen, Göttingen, Germany, 1996.
47 G. M. Sheldrick, *SHELXS*, University of Göttingen, Göttingen, Germany, 1997.
48 M. C. Burla, M. Camalli, B. Carrozzini, G. L. Cascarano, C. Giacovazzo, G. Polidoria and R. Spagnab, *J. Appl. Crystallogr.*, 2003, **36**, 1103.
49 P. v. d. Sluis and A. L. Spek, *Acta Crystallogr., Sect. A: Found. Crystallogr.*, 1990, **46**, 194.
50 A. L. Spek, *J. Appl. Crystallogr.*, 2003, **36**, 7.
51 M. Q. T. Tran, Y. Nygren, C. Lundin, P. Naredi and E. Bjorn, *Anal. Biochem.*, 2010, **1**, 76.